Available online at www.sciencedirect.com
SCIENCE DIRECT®
Phytochemistry 67 (2006) 1460–1475
PHYTOCHEMISTRY
www.elsevier.com/locate/phytochem

Robustness of central carbohydrate metabolism in developing maize kernels

Gertraud Spielbauer [a,1], Lilla Margl [a,1], L. Curtis Hannah [c], Werner Römisch [b], Christian Ettenhuber [b], Adelbert Bacher [b], Alfons Gierl [a], Wolfgang Eisenreich [b], Ulrich Genschel [a,*]

[a] *Lehrstuhl für Genetik, Technische Universität München, Am Hochanger 8, 85350 Freising, Germany*
[b] *Lehrstuhl für Organische Chemie und Biochemie, Technische Universität München, Lichtenbergstrasse 4, 85747 Garching, Germany*
[c] *Horticultural Sciences Department, University of Florida, Gainesville, FL 32611, USA*

Received 20 March 2006; received in revised form 22 May 2006
Available online 3 July 2006

Abstract

The central carbohydrate metabolism provides the precursors for the syntheses of various storage products in seeds. While the underlying biochemical map is well established, little is known about the organization and flexibility of carbohydrate metabolic fluxes in the face of changing biosynthetic demands or other perturbations. This question was addressed in developing kernels of maize (*Zea mays* L.), a model system for the study of starch and sugar metabolism. ^{13}C-labeling experiments were carried out with inbred lines, heterotic hybrids, and starch-deficient mutants that were selected to cover a wide range of performances and kernel phenotypes. In total, 46 labeling experiments were carried out using either [U-$^{13}C_6$]glucose or [U-$^{13}C_{12}$]sucrose and up to three stages of kernel development. Carbohydrate flux distributions were estimated based on glucose isotopologue abundances, which were determined in hydrolysates of starch by using quantitative ^{13}C-NMR and GC-MS. Similar labeling patterns in all samples indicated robustness of carbohydrate fluxes in maize endosperm, and fluxes were rather stable in response to glucose or sucrose feeding and during development. A lack of ADP-glucose pyrophosphorylase in the *bt2* and *sh2* mutants triggered significantly increased hexose cycling. In contrast, other mutations with similar kernel phenotypes had no effect. Thus, the distribution of carbohydrate fluxes is stable and not determined by sink strength in maize kernels.

Keywords: *Zea mays*; Starch mutants; Heterotic hybrids; Central carbohydrate metabolism; Flux patterns; Metabolic robustness

1. Introduction

Metabolic flux analysis is a component of functional genomics that is complementary to the description of cellular inventory attained by current steady state expression profiling and metabolic profiling techniques (Fernie et al., 2005). Although it is generally agreed that flux analysis is essential for understanding plant metabolism it is still an emerging area in the plant sciences (Roscher et al., 2000; Ratcliffe and Shachar-Hill, 2001; Kruger et al., 2003; Schwender et al., 2004). Currently, it is not possible to predict the outcome of metabolic engineering approaches in plants. In contrast, steady state flux analysis in microbes already provided an understanding of metabolic networks that helped to identify successful metabolic engineering strategies and enabled rational pathway design (Ratcliffe and Shachar-Hill, 2006).

Only few large-scale metabolic flux maps of plant tissues are available so far, e.g. from maize root tips (Dieuaide-Noubhani et al., 1995), tomato cells in suspension culture (Rontein et al., 2002), developing soybean embryos (Sriram et al., 2004), and developing *Brassica napus* embryos (Schwender et al., 2003, 2004). However, no comparative

* Corresponding author. Tel.: +49 8161 715644; fax: +49 89 715636.
E-mail address: genschel@wzw.tum.de (U. Genschel).
[1] These authors contributed equally to this work.

0031-9422/$ - see front matter © 2006 Elsevier Ltd. All rights reserved.
doi:10.1016/j.phytochem.2006.05.035

metabolic flux analysis has been carried out in plants so far. In this study, we applied stable isotope labeling to maize (*Zea mays* L.) kernels from nine different starch-deficient mutants, five inbred lines, and heterotic hybrids (summarized in Table 1). Our analysis of this set of samples, which comprises considerable variation with respect to the capacity for starch biosynthesis and kernel composition, allowed us to address the effect of carbon source, developmental stage, and sink strength on metabolic fluxes involved in hexose cycling.

The availability of numerous maize mutants that affect the quality and quantity of carbohydrates in seeds has established maize as a model system to investigate the biosynthesis of starch (reviewed in Nelson and Pan, 1995; Kossmann and Lloyd, 2000; Boyer and Hannah, 2001). The metabolic map in Fig. 1 shows the core steps for conversion of sucrose to starch in cereal endosperm and indicates the biochemical lesions in the mutants included in this study.

Maize kernels use sucrose from source leaves as building blocks for starch biosynthesis. Incoming sucrose is cleaved either by sucrose synthase to yield UDP-glucose and fructose or by invertase, which cleaves sucrose in an irreversible manner into glucose and fructose (Winter and Huber, 2000). Mutations in *Sh1* and *Sus1*, which encode the two sucrose synthase isozymes in maize endosperm (Chourey, 1981; Echt and Chourey, 1985) condition mild kernel phenotypes associated with 22% and 47% reductions in the starch content of the *sh1* single and the *sh1sus1* double mutants, respectively (Chourey et al., 1998). In contrast, the loss of cell wall-bound invertase in the *mn1* mutants leads to severe kernel phenotypes characterized by 70–80% reduction of seed weight (Cheng et al., 1996).

Table 1
Summary of ^{13}C-labeling experiments with developing maize kernels carried out in this study

Maize line	Biochemical lesion	Labeling interval (carbon source)
W64A		15–22 DPP (glc, suc)
sh1	Sucrose synthase	15–22 DPP (glc, suc)
bt1	Adenylate translocator	15–22 DPP (glc, suc)
bt2	AGPase (small subunit)	15–22 DPP (glc, suc)
ae	SBEIIb	15–22 DPP (glc, suc)
wx	GBSSI	15–22 DPP (glc, suc)
su1	DBE	15–22 DPP (glc, suc)
W22		15–22 DPP (glc, suc)
mn1	Invertase	15–22 DPP (glc, suc)
sh1 sus1	Sucrose synthase	15–22 DPP (glc, suc)
Fa56		15–22 DPP (glc, suc)
sh2	AGPase (large subunit)	15–22 DPP (glc, suc)
Sh2-Rev6		15–22 DPP (glc, suc)
Mo17		11–18 (glc), 18–25 (glc, suc), 25–32 DPP(glc)
B73		11–18 (glc), 18–25 (glc, suc), 25–32 DPP(glc)
B73 × Mo17 (F1)		11–18 (glc), 18–25 (glc), 25–32 DPP (glc)
B73 × Mo17 (F2)		11–18 (glc), 18–25 (glc, suc), 25–32 DPP (glc)
Mo17 × B73 (F1)		11–18 (glc), 18–25 (glc), 25–32 DPP (glc)
Mo17 × B73 (F2)		11–18 (glc), 18–25 (glc), 25–32 DPP (glc)

Kernel mutants are listed below the inbred line corresponding to their genetic background. For abbreviations of enzyme names see Introduction or legend of Fig. 1. *suc*, labeling with [U-$^{13}C_{12}$]sucrose; *glc*, labeling with [U-$^{13}C_6$]glucose.

The cleavage products of sucrose synthase or invertase are converted into glucose-1-phosphate by the action of hexokinase, phosphoglucomutase, phosphoglucoisomerase, and UDP-glucose pyrophosphorylase (UGPase). Glucose-1-phosphate is utilized by ADP-glucose pyrophosphorylase (AGPase) to produce ADP-glucose, the key step of starch synthesis. The small and large subunits of AGPase are encoded by the *Brittle-2* (*Bt2*) and *Shrunken-2* (*Sh2*) genes, respectively (Bae et al., 1990; Bhave et al., 1990). In wild-type maize endosperm, the major activity of AGPase is localized in the cytosol, with a minor activity in the amyloplast (Denyer et al., 1996). Cytosolic ADP-glucose is supposed to be transported into the amyloplast by the amyloplast membrane protein Brittle1 (BT1) (Sullivan and Kaneko, 1995; Shannon et al., 1998). Mutations effecting the synthesis or transport of ADP-glucose result in severe kernel phenotypes. Loss of *Bt1*, *Bt2*, or *Sh2* functions conditions similar kernel phenotypes, marked by 70–80% lower starch contents and much increased concentrations of soluble sugars (Hannah et al., 1993). In contrast, the revertant *Sh2-Rev6* shows 11–18% increased seed weight due to an altered AGPase with reduced sensitivity to phosphate inhibition (Giroux et al., 1996).

In the amyloplast, starch is synthesized from ADP-glucose by the concerted action of multiple isoforms of starch synthases, starch branching enzymes, and starch debranching enzymes. Mutations affecting starch-synthesizing enzymes lead to milder kernel phenotypes with altered ratios of the two main starch components, amylose and amylopectin, while the total amounts of polysaccharides are not changed dramatically. In *amylose extender (ae)* endosperm, the relative amount of amylose is increased due to a lack of starch branching-enzyme IIb (SBEIIb) (Boyer and Preiss, 1978). In contrast, *waxy (wx)* mutants lack granule-bound starch-synthase I (GBSSI) and have starches solely composed of amylopectin (Nelson and Rines, 1962). The *Sugary-1* (*Su1*) gene encodes an isoamylase-type debranching-enzyme (James et al., 1995), which is involved in amylopectin synthesis. In addition to starch, *su1* kernels accumulate a second type of polyglucan, the highly branched water-soluble phytoglycogen at the expense of amylopectin (Wang et al., 1993).

Hybrid crosses between inbred lines exhibit heterosis (hybrid vigor), which refers to increased biomass production and other superior traits compared with the better of the two parents (Birchler et al., 2003). Crosses of maize inbred lines belonging to the Stiff Stalk Synthetic group (e.g. B73) with lines from the Lancaster open-pollinated population (e.g. Mo17) result in hybrids that show an approximately 2.5-fold yield-increase over the parental

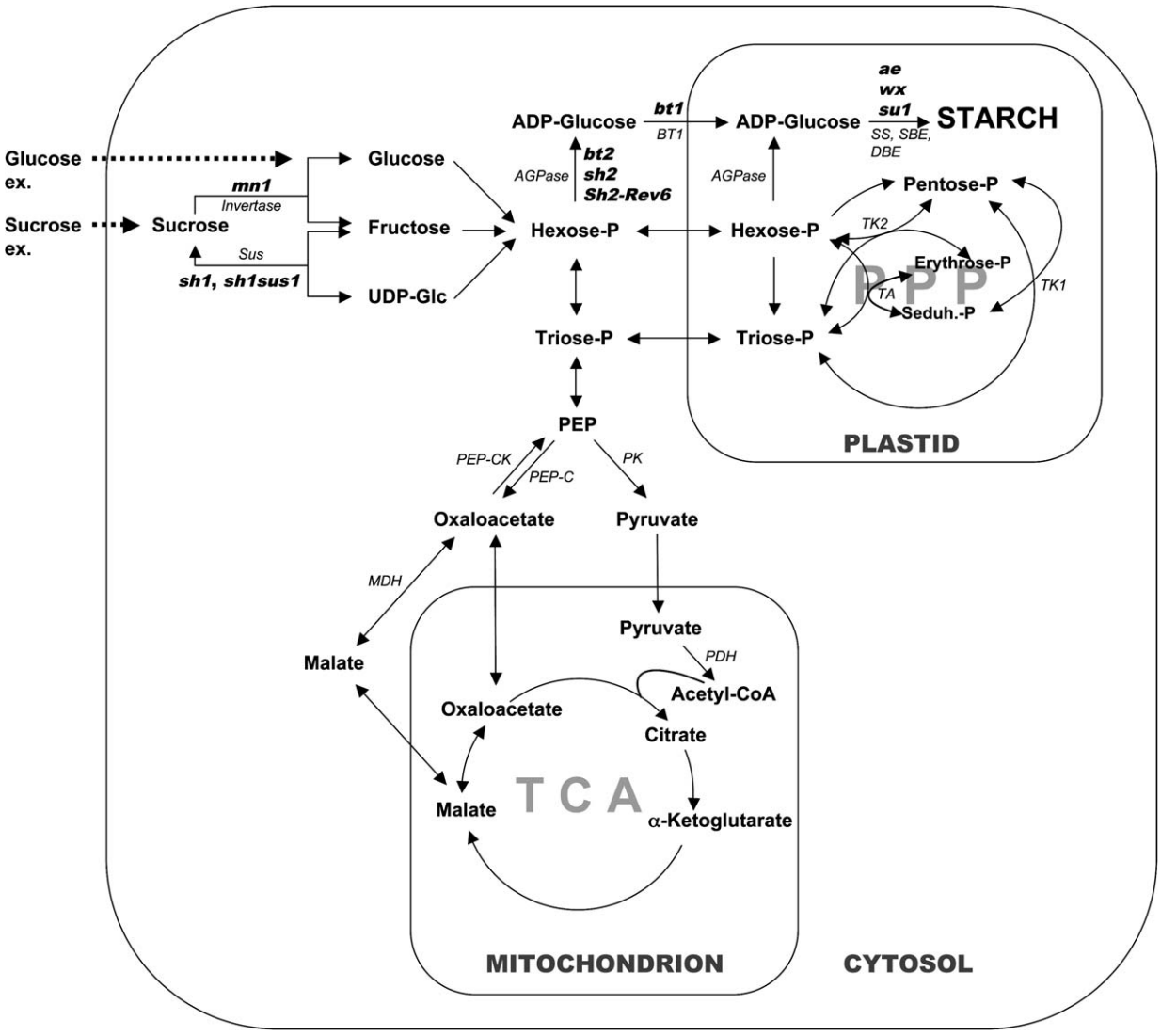

Fig. 1. Pathways of the central carbohydrate metabolism in developing maize kernels. The map is based on the recent literature on maize or higher plant biochemistry. Starch-deficient mutants are shown in boldface type next to the affected reaction step. *ae*, amylose extender; *bt*, brittle; *mn*, miniature; *sh*, shrunken; *su*, sugary; *sus*, sucrose synthase; *wx*, waxy; *AGPase*; ADP-glucose pyrophosphorylase; *DBE*, starch debranching enzyme; *MDH*, malate dehydrogenase; *PEP-C*, PEP carboxylase; *PEP-CK*, PEP carboxykinase; *PDH*, pyruvate dehydrogenase; *PK*, pyruvate kinase; *SBE*, starch branching enzyme; *SS*, starch synthase; *TA*, transaldolase; and *TK*, transketolase.

lines (Moreno-Gonzales and Dudley, 1981). Specifically, the B73 × Mo17 hybrid is recognized for its exceptional performance and was widely grown in the late 1970s and early 1980s (Wolf and Hallauer, 1997). Thus, the genetic constitutions included in this study are associated with decreased sink strength in case of the kernel mutants or increased sink strength in case of the heterotic hybrids.

Numerous studies have demonstrated that mutations in the above-mentioned genes have effects beyond the starch biosynthetic pathway and result in profound changes in kernel physiology and metabolism as a whole. Most of these mutants have been extensively studied for their effects on storage compounds (Creech, 1968; Lee and Tsai, 1985), metabolite levels (Creech, 1968; Tobias et al., 1992; Shannon et al., 1996), enzyme activities (Doehlert and Kuo, 1990; Singletary et al., 1997), and transcript amounts (Doehlert and Kuo, 1994; Giroux et al., 1994). These studies imply that mutations in the starch pathway lead to alterations in the primary carbohydrate metabolism, i.e. glycolysis, pentose phosphate pathway (PPP), and tricarboxylic acid (TCA) cycle.

Stable isotope labeling, which has evolved as an important tool in the study of plant metabolic networks (Kruger et al., 2003; Schwender et al., 2004), was used to characterize the primary carbohydrate metabolism in developing maize kernels. Applying [U-$^{13}C_6$]glucose to cultured maize kernels, we analyzed previously the isotopomer composition of amino acids, triglycerids, sitosterol, and glucosyl units derived from starch (Glawischnig et al., 2001, 2002). Based on an improved method for the determination of glucose isotopologue abundances (Eisenreich et al., 2004), we recently used the full glucose isotopologue distribution

to quantify the contribution of glycolysis, the pentose phosphate pathway (PPP), and the tricarboxylic acic (TCA) cycle to the processing of glucose in developing maize kernels (Ettenhuber et al., 2005). We report here the response of metabolic fluxes in a series of important maize mutants. The aim of this study was to compare relative fluxes of the central carbohydrate network in starch-deficient mutants and other maize lines that represent various disparate phenotypes. We worked on the hypothesis that the large pleiotropic effects of the starch-deficient mutants and the large differences in the performances of mutant and heterotic maize lines would result in a shift of relative fluxes through the principal pathways of the central carbohydrate network. To our surprise, the glucose labeling patterns in the majority of genotypes were essentially identical, and only the *bt2* and *sh2* mutants showed changes in the carbohydrate flux pattern. This indicates high stability of the central carbohydrate metabolism in maize endosperm.

2. Results

2.1. Rationale of ^{13}C-labeling experiments

The qualitative and quantitative interpretation of labeling data requires a model of the metabolic network. Apart from sugar uptake and starch biosynthesis (see Section 1), our network contains the principal pathways of primary carbohydrate metabolism, i.e. glycolysis, PPP, TCA cycle, and gluconeogenesis (Fig. 1). These pathways cause specific redistributions of ^{13}C-label in carbohydrate intermediates, respectively. Therefore, their relative activities can be inferred from the ^{13}C-pattern of glucose incorporated into starch during a labeling experiment. Consequently, we treat the glucose labeling pattern as a phenotype of the underlying fluxes and use this pattern to diagnose changed fluxes in response to perturbation.

The map in Fig. 1 is based on recent literature on maize or higher plant biochemistry and the KEGG database (Plaxton, 1996; Buchanan et al., 2000; Kruger and van Schaewen, 2003; Tetlow et al., 2004; Kanehisa et al., 2006). In case of the PPP, the nonoxidative part consists of three reversible transformations, the transketolase 1, transketolase 2, and the transaldolase reactions. Additional transaldolase and transketolase reactions were proposed by van Winden et al. (2001) but not incorporated into our model. Carbon can enter the TCA cycle in the form of glycolysis-derived acetyl-CoA or, via anaplerotic reactions, in the form of oxaloacetate or malate. However, on the basis of [U-$^{13}C_6$]glucose labeling data, it is not possible to distinguish between these alternatives because they result in the same set of glucose isotopologues.

The detection of the glucose isotopologues {011000} and {000110} indicates the simultaneous operation of glycolysis, TCA cycle, and gluconeogenesis in maize kernels during the labeling period. The backward flux of carbon from TCA cycle intermediates to the hexose phosphate pool requires the enzyme PEP carboxykinase, which catalyses the reversible decarboxylation of oxaloacetate to yield PEP. The expression of this enzyme in maize endosperm has not been described so far, but it is known to be widely distributed in the plant kingdom with well known functions in gluconeogenesis of germinating seeds and in photosynthesis of C4 and some CAM plants (Lea et al., 2001). The glucose isotopologue distributions observed in maize kernels in this study (see below) provide the first evidence for the simultaneous action of the antagonistic enzymes PEP carboxylase and PEP carboxykinase or the simultaneous action of glycolysis and gluconeogenesis during active starch deposition.

Our interpretation of the labeling data is based on the assumption that isomerase and epimerase reactions among hexose phosphates, pentose phosphates, and triose phosphates are fast and in near-equilibrium (Katz and Rognstad, 1967). Accordingly, glucose-6-phosphate, glucose-1-phosphate, and fructose-6-phosphate are treated as one hexose phosphate pool, ribose-5-phosphate, ribulose-5-phosphate, and xylulose-5-phosphate are treated as one pentose phosphate pool, and dihydroxyacetone phosphate (DHAP) and glyceraldehyde-3-phosphate (GAP) are treated as one triose phosphate pool. The assumption of triose phosphate and pentose phosphate pools in maize endosperm is supported by amino acid labeling patterns we published earlier (Glawischnig et al., 2001). Firstly, similar isotopic compositions of the C1–C3 carbon atoms of phenylalanine and tyrosine, which are derived from cytosolic PEP, and of triacylglyceride-derived glycerol, which is derived from plastidic DHAP, indicate that the cytosolic PEP and plastidic DHAP pools are in near-equilibrium. Secondly, the isotopologue pattern of histidine reveals a nearly complete cleavage between carbon C2 and C3 in ribose-5-phosphate. This shows that interconversion of pentose phosphates is fast compared with flux through the oxidative part of the PPP (Szyperski, 1995). The assumption of one hexose phosphate pool cannot be directly inferred from our data, but is justified by previous reports on hexose phosphate pools in maize, tomato, and *Brassica napus* (Dieuaide-Noubhani et al., 1995; Rontein et al., 2002; Schwender et al., 2003).

Interpretation of our isotope-labeling data in terms of metabolic fluxes requires that the experimental system is in metabolic and isotopic steady state (Roscher et al., 2000). Assuming that the turnover of starch in maize endosperm is low compared with the rate of starch deposition, the labeling of glucose derived from hydrolyzed starch represents an integral value over the total incubation time in our system, and this includes the period necessary for the initial isotopic equilibration of metabolites. In order to ensure that labeling to isotopic steady state was achieved and that no large changes of the isotopic state during the labeling period occurred, glucose from the outer layers of *su1*-starch was compared to completely hydrolyzed *su1*-starch. Partial hydrolysis of *su1*-starch from an

[U-$^{13}C_6$]glucose labeling experiment yielded a glucose fraction with an absolute ^{13}C-enrichment of 2.50%, which is close to the value for soluble sugars (2.56%) in the same experiment and significantly higher than the value for completely hydrolyzed *su1*-starch (2.23%), indicating that only recently synthesized starch was degraded (Keeling et al., 1988). The isotopologue pattern obtained for recently synthesized *su1*-starch is highly similar to the pattern representing the entire labeling period (data not shown), suggesting that the time span required to establish isotopic steady state was short compared with the total labeling time and that isotopic and metabolic steady state was maintained throughout the experiment.

2.2. Kernel culture

Developing maize kernels in the main phase of starch accumulation were grown in sterile culture and supplied with [U-$^{13}C_6$]glucose or [U-$^{13}C_{12}$]sucrose and a 30-fold excess of the same sugar without ^{13}C-label (natural abundance), respectively. After an incubation period of 7 days, starch was isolated, degraded enzymatically to glucose, and the isotopologue patterns of the purified glucose samples were determined as described in the Experimental section. In addition, phytoglycogen was isolated from *su1* kernels and treated in the same way. The mutant kernels used in this study were present in the genetic backgrounds of the inbred lines W64A (*ae*, *wx*, *su1*, *sh1*, *bt1*, *bt2*), W22 (*mn1*, *sh1 sus1*), and Fa56 (*Sh2-Rev6*, *sh2*). Mutant kernels and their corresponding wildtypes were labeled between 15 and 22 DPP only, while Mo17, B73, and their F1 hybrids (B73 × Mo17 and Mo17 × B73) and F2 progeny (derived from the F1 hybrids by selfing) were labeled during three consecutive intervals (11–18 DPP, 18–25 DPP, 25–32 DPP) (Table 1). In the following, individual samples are identified by the genotype of the kernels and the carbon source (glc or suc) used for ^{13}C-labeling, respectively. The *in vitro* culture method for intact maize seeds used in this study supports kernel development to maturity and subsequent germination (Gengenbach, 1977), and phenotypes of kernel mutants are similar on the cob and in culture (Cheng and Chourey, 1999; this study). Thus, while artefactual observations caused by the *in vitro* culture process cannot be excluded, our experimental system is likely to reflect the situation *in vivo*.

The ratio of labeled to unlabeled sugars in the culture medium was 1:30, which is substantially lower than the ratio in other ^{13}C-labeling experiments with plants, where typically a 1:10 isotopic dilution was used (e.g. Schwender et al., 2003; Sriram et al., 2004). A high dilution of label allows to neglect all glucose isotopologues, which can be formed only by recombination of labeled fragments. The number of possible glucose isotopologues can thus be constrained to 21, allowing the determination of the entire ^{13}C-isotopologue distribution of glucose by analyzing multiplet structures in proton-decoupled ^{13}C-NMR spectra (Eisenreich et al., 2004).

The global ^{13}C-enrichment in the starch fraction at the end of the labeling period depends on the amount of preformed starch, which contains glucose at natural ^{13}C-abundance, and the amount of starch synthesized during the ^{13}C-labeling period. Using isotope ratio mass spectrometry (IRMS), we obtained ^{13}C-enrichments ranging from 1.55% to 2.81% in our samples. This reflects labeling at different kernel stages or differences in the speed of kernel development and in patterns of starch accumulation, which are known to occur in several kernel mutants (Singletary et al., 1997). In order to enable direct comparison of isotopologue patterns obtained from samples with different global ^{13}C-enrichments, the absolute isotopologue abundances need to be normalized. To this end, the excess isotopologue abundances (Supplemental Table 1) were normalized to the ^{13}C-enrichment above natural abundance considering the number of labeled atoms of each isotopologue as described in the Experimental section. This value was termed the percentage ^{13}C-fraction and represents the fraction of excess ^{13}C-label stored in a given isotopologue.

2.3. Evaluation of ^{13}C-labeling patterns

In total, 48 glucose isotopologue patterns were obtained from 46 independent labeling experiments on 19 different maize genotypes, and the actual isotopologue concentrations were normalized to the percentage ^{13}C-fraction. The resulting glucose isotopologue patterns were similar in all samples (Fig. 2), clearly showing that no massive reprogramming of carbohydrate fluxes occurs in any of the lines analyzed. In order to detect less obvious outliers, principal component analysis (PCA) was performed with the normalized isotopologue data shown in Fig. 2. This approach grouped the vast majority of samples in a single cluster supporting the conclusion that the patterns are highly related (Fig. 3). However, the *bt2* and *sh2* samples cosegregate and cluster separately in PCA. This provides a hint that a block in AGPase, which is encoded by *Bt2* and *Sh2*, leads to modified carbohydrate fluxes. Other potential outliers were *wx*-suc, *ae*-suc, and two samples labeled late in kernel development (25–32 DPP). The significance of these outliers is not clear, though, because related samples (i.e. *wx*-glc, *ae*-glc, and other samples labeled at 25–32 DPP) are inconspicuous.

The effects on the isotopologue labeling pattern, that were caused by carbon source, kernel development, or a block in AGPase, were analyzed by using the paired *t*-test or repeated-measures analysis of variance (ANOVA) (Fig. 4). Based on the 17 genotypes that were labeled with [U-$^{13}C_6$]glucose and [U-$^{13}C_{12}$]sucrose, respectively, no individual isotopologue was changed by more than 10%, indicating that there was only a minor difference between glucose or sucrose as the carbon source in the kernel culture (Fig. 4A). However, kernels grown on sucrose consistently show higher amounts of the {111111} isotopologue and decreased amounts of {110000} and {000011}, so

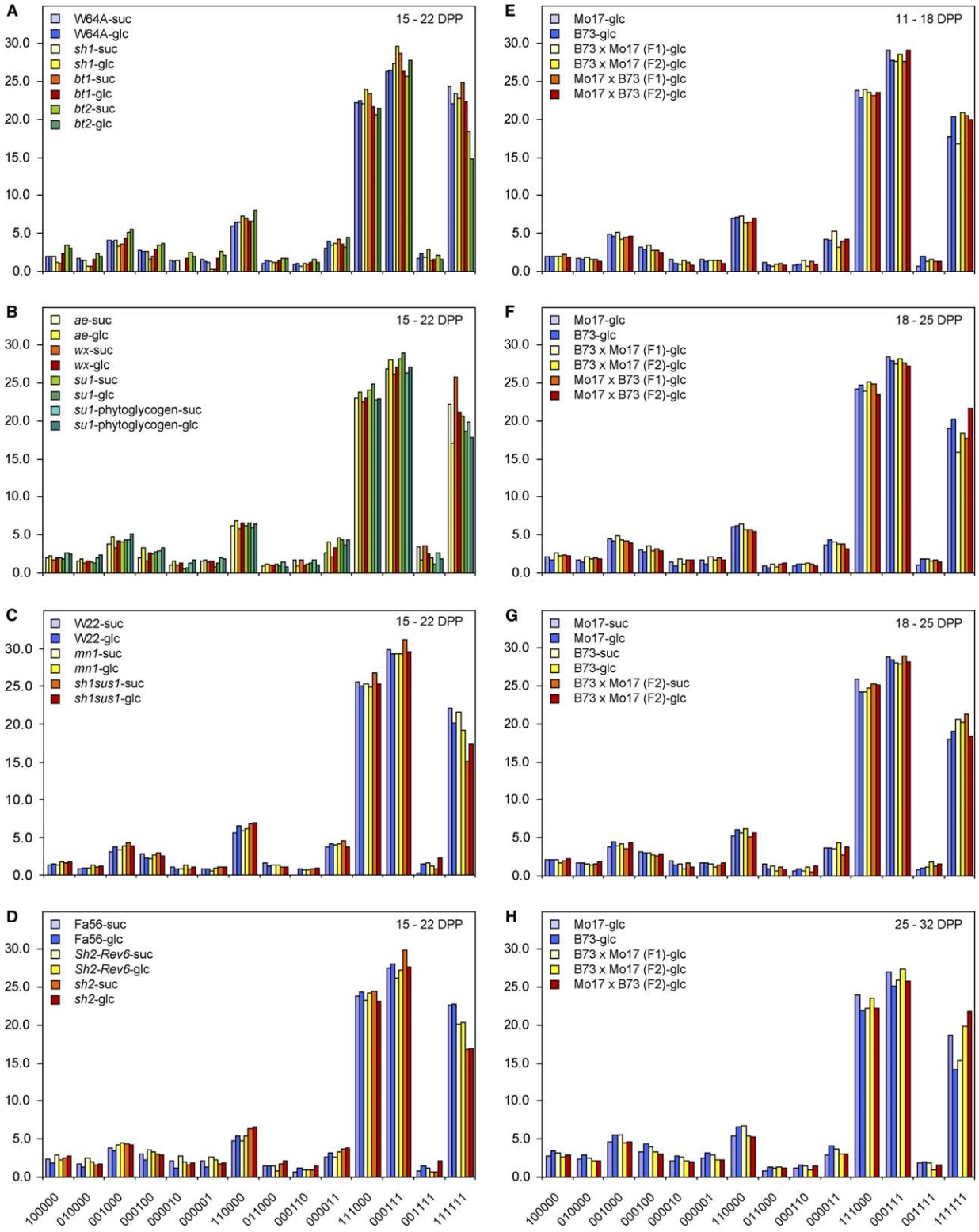

Fig. 2. Glucose isotopologue patterns. Maize kernels were labeled for 7 days with [U-$^{13}C_6$]glucose or [U-$^{13}C_{12}$]sucrose, respectively. Glucose isotopologue abundances from starch and phytoglycogen (in case of *su1* kernels) hydrolysates were determined as described in the Experimental section (data provided in Supplementary Table 1). Isotopologue abundances were normalized to percentage ^{13}C-fractions, which signify the fractions of ^{13}C-label associated with each isotopologue. Mutants in the W64A (A, B), W22 (C), and Fa56 (D) backgrounds are shown together with their corresponding wildtype lines. Isotopologue patterns obtained from Mo17, B73, and heterotic hybrid crosses between the two lines were ordered by the labeling period. For these lines, labeling was performed at 11–18 DPP (E), 18–25 DPP (F, G), and 25–32 DPP (H). The samples are named according to genotype and the carbon source in the medium. Common abbreviations are used for starch-deficient mutants (see Section 1 and Fig. 1). Glucose isotopologues are named as described in the Experimental section. *suc*, labeling with [U-$^{13}C_{12}$]sucrose; *glc*, labeling with [U-$^{13}C_6$]glucose.

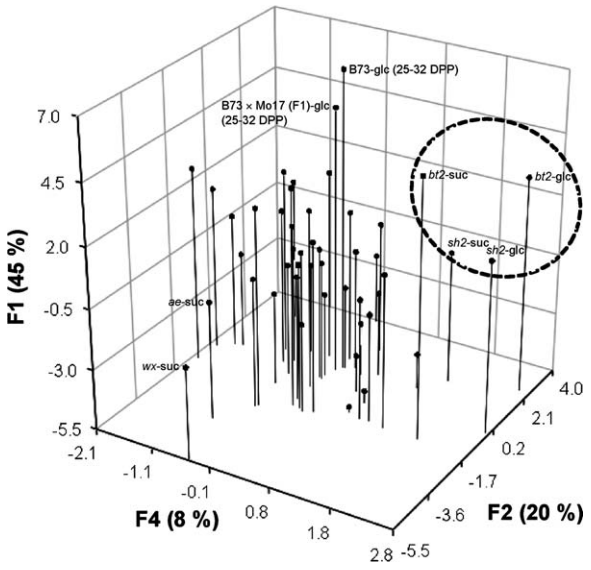

Fig. 3. Clustering of isotopologue patterns. Principal component analysis (PCA) was performed with the normalized isotopologue data of 48 samples in order to identify genotypes with altered carbohydrate metabolism. Isotopologue patterns of the *bt2* and *sh2* mutants cosegregate and cluster separately from the majority of samples. PCA factors 1, 2, and 4 were chosen for best visualization of clusters and represent 63% of the variability present in the initial dataset.

the data can be interpreted in terms of a decreased ratio of hexose cycling over net starch deposition in response to sucrose. Possible explanations for such a change include decreased activity of reactions participating in glucose cycling, increased flux into starch, or decreased turnover of starch.

Previously, we reported small changes of carbohydrate fluxes during kernel development of the W22 maize inbred (Ettenhuber et al., 2005). In this study, labeling data from three different developmental stages (11–18 DPP, 18–25 DPP, and 25–32 DPP) are available for five genotypes including the inbred lines B73, Mo17, and their F1 and F2 progeny (Fig. 4B). Repeated-measures ANOVA identified several isotopologues whose ^{13}C-fractions changed slightly during kernel development. Post-tests following ANOVA revealed a pattern of high similarity between the 11–18 DPP and 18–25 DPP groups, which differed from the 25 to 32 DPP group. However, there was no significant matching between the three groups and no consistent trend of isotopologue changes over developmental time could be identified. Thus, the carbohydrate flux distribution remains essentially constant for the major part of kernel development and small changes may occur late in development.

In order to further test the hypothesis that mutants lacking AGPase have modified carbohydrate fluxes, ^{13}C-fractions of glucose isotopologues were compared between the *bt2* and *sh2* samples and their respective wildtypes (Fig. 4C). Significant differences were obtained for three isotopologues carrying ^{13}C-label in the positions C-1 to C-3 of the glucose molecule but not for isotopologues labeled only in positions C-4 to C-6. This points to changes in the activity of the PPP which is known to act only on the upper part of the glucose molecule (Portais and Delort, 2002). Additionally, *bt2* and *sh2* showed a greater than 25% reduction in the amounts of {111111} glucose, which points to increased activity of processes involved in hexose cycling relative to net starch synthesis. The increase of {110000} glucose and concomitant decrease in {111000} and {111111} observed in the *bt2* and *sh2* samples (Fig. 4C) is completely consistent with the corresponding NMR spectra (Fig. 5). A detailed inspection of normalized ^{13}C-NMR signal intensities for C-1β shows differences between samples obtained from the *bt2* mutant and those from the corresponding W64A wildtype line in both labeling experiments (i.e. with [U-$^{13}C_6$]glucose or [U-$^{13}C_{12}$]sucrose as a tracer). On the other hand, the normalized signal intensities of the same satellite signals were in perfect agreement between the *bt1* mutant and the corresponding W64A wildtype. Specifically, the satellite pairs reflecting the {111XX0} and {111XX1} isotopologue groups were lower in the signals of the *bt2* mutant (shown in red) as compared to the signals of the corresponding wildtype line (shown in green). Since the {111XX1} group is indicative of the {111111} isotopologue of glucose in our experimental set-up, it can be concluded that hexose cycling is increased in the *bt2* mutant, but not in the *bt1* mutant. Similarly, the C-1β signals reflecting the amount of [U-$^{13}C_6$]glucose were also detected with lower normalized intensities in the samples from the *sh2* mutants as compared to the corresponding signals of the samples from the Fa56 wildtype line (not shown).

Glucose isotopologue abundances can be interpreted in terms of carbohydrate fluxes by assigning individual isotopologues to specific processes of the carbohydrate metabolism as previously described (Glawischnig et al., 2002; Ettenhuber et al., 2005). Given the high isotopic dilution of ^{13}C-sugars supplied in the medium (see above), the recovery of uniformly labeled glucose {111111} represents the fraction of glucose incorporated into starch without prior fragmentation. Averaging all experiments in this study, the {111111} isotopologue accounts for 20.2% ± 2.6% (mean ± SD) of the excess ^{13}C-label incorporated into starch. Thus, at face value, approximately 20% of the glucose molecules taken up from the culture medium were channeled directly into starch, while 80% underwent fragmentation. However, this is an upper estimate for direct flux into starch and a lower estimate for the entry of glucose into glycolysis or the PPP, respectively. This is due to the fact that ^{13}C-labeled intermediates of glycolysis, PPP, and the TCA cycle, from which partially labeled hexoses are synthesized, are also subject to processes like amino acid biosynthesis or respiration, which recruit carbohydrate intermediates into sinks other than starch biosynthesis. The central carbohydrate metabolism of maize kernels is characterized by high relative fluxes between the hexose phosphate and triose phosphate pools. This is

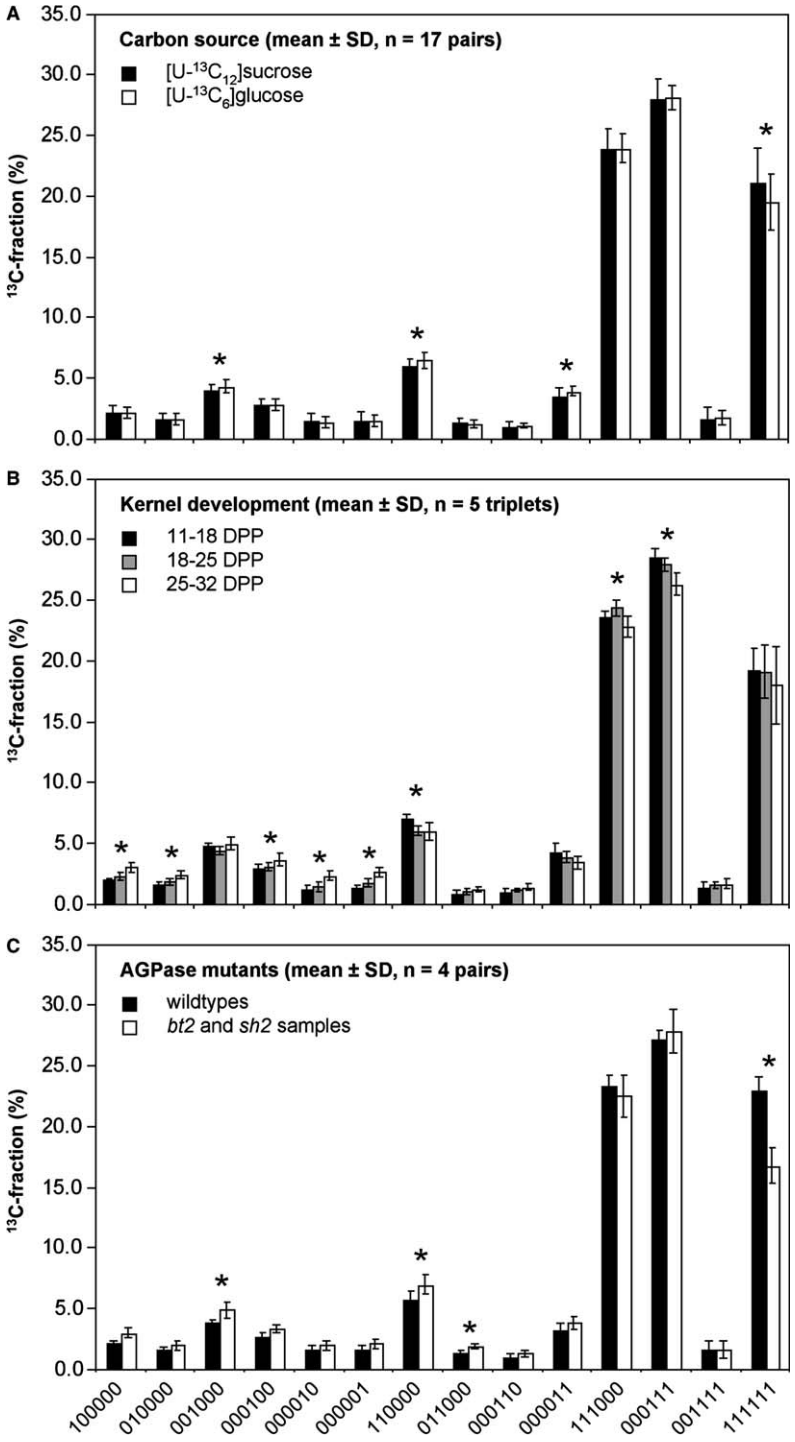

Fig. 4. Response of glucose isotopologue patterns to carbon source, developmental stage, and mutations in AGPase. The glucose labeling patterns shown in Fig. 2 were queried for specific responses to carbon source (A), developmental stage (B), or to lack of AGPase (C). This analysis was performed with pairs or triplets of samples that differ only in one aspect, respectively. Sample pairs like *wx*-suc/*wx*-glc were selected to test the response to carbon source. Similarly, developmental trends were analyzed based on triplets of samples with the same genotype but labeled at three different stages (DPP 11–18/DPP 18–25/DPP 25–32). Finally, wildtype-mutant pairs like W64A-glc/*bt2*-glc were chosen to characterize the response due to loss of AGPase. The paired *t*-test (A, C) or repeated-measures analysis of variance (ANOVA) (B) were then used to compare matched sets of experiments. Glucose isotopologues with significantly changed mean ^{13}C-fractions (p-value < 0.05) are marked with an asterisk.

shown by high amounts of the {111000} and {000111} isotopologues, which can be assumed to be due mainly to hexose-triose-cycling and together account for 46–58% of the ^{13}C-label recovered in starch. The PPP is also a dominant process involved in shaping glucose isotopologues and mainly associated with the production of the isotopologues {110000}, {000011}, {001000}, and {000100}. The isotopologues {011000} and {000110} are exclusively

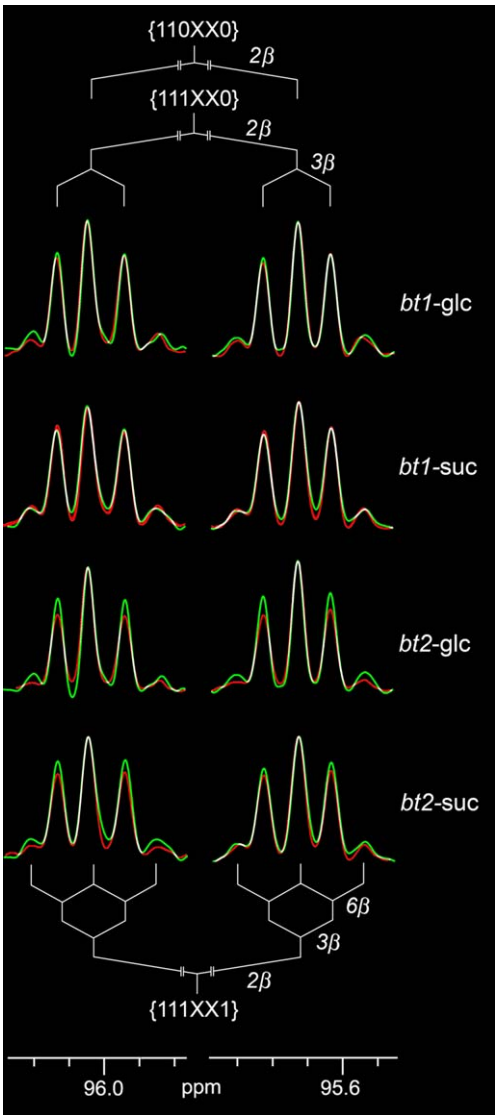

Fig. 5. Overlay of C-1β satellite signals from ^{13}C NMR spectra of *bt1*, *bt2*, and W64A starch-glucose. The signals of the mutants *bt1* and *bt2* (red lines) and the corresponding W64A wildtype genetic background (green lines) are shown in dual mode. Note that a perfect overlap of green and red results in white. Signals reflecting the isotopologue group {110XX0} (i.e. the middle peak of each signal group) were scaled to the same size in order to allow direct comparison of NMR spectra from samples with different global ^{13}C-enrichments. The satellites represent different multiply ^{13}C-labeled glucose isotopologues as indicated by the ^{13}C-coupling patterns. Therefore, differences in satellite-to-satellite ratios correspond to differences in specific glucose isotopologue ratios. The isotopologue groups {110XX0}, {111XX0}, and {111XX1} represent the specific glucose isotopologues {110000}, {111000}, and {111111}, respectively.

formed by reactions of the TCA cycle and subsequent gluconeogenesis. They account for less than 4% of excess ^{13}C-label, indicating a minor gluconeogenetic flux.

^{13}C-labeling data were also interpreted quantitatively by estimating the participation of five cyclic pathways in hexose cycling as previously described (Ettenhuber et al., 2005). The distributions of these metabolic processes, that consume and regenerate hexoses, were obtained from 48 isotopologue patterns, respectively. Averaging the calculated patterns of hexose cycling resulted in small standard deviations for each process (Fig. 6A). This shows that the overall pattern of carbohydrate fluxes is stable and that the mutations included in this study have no large effect in this respect: interconversion of hexose phosphates by glycolytic reactions (*emp*) and reactions of the PPP (*ppp1* and *ppp2*) are the dominant processes of carbohydrate metabolism in maize endosperm, while the TCA cycle followed by gluconeogenesis (*tca*) contributes much less to overall glucose cycling. While this general pattern is also conserved in mutants lacking AGPase, comparison of the *bt2* and *sh2* samples with their corresponding wildtypes revealed a significant effect (Fig. 6B). AGPase mutants show a 30% reduction of direct incorporation of glucose into starch (*dtr*), and the additional hexose cycling implicated in this result is mostly exerted via the nonoxidative part of the PPP (*ppp2*).

2.4. Stability of key metabolic branch points

As fluxes through the pathways of the primary carbohydrate metabolism (glycolysis, PPP, and TCA cycle) result in the formation of different, pathway-typical glucose isotopologues, specific ratios between individual isotopologues can be used to roughly describe basic features of carbon metabolism. The ratios of the isotopologue pairs {111000} vs. {000111} and {111000} vs. {110000} can be used to estimate the rigidity of the flux split at the branch point between glycolysis and PPP. Starting from [U-$^{13}C_6$]glucose, glycolytic reactions produce the isotopologues {111000} and {000111} in equal amounts. The excess of the {000111} over the {111000} isotopologue, which was observed in every sample, can be explained by the transaldolase forward reaction, which generates the {000111}, but not the {111000} isotopologue (Ettenhuber et al., 2005). Likewise, the isotopologue {110000} is considered an indicator of the PPP, because it is generated mainly by the transketolase 1 reaction of xylulose-5-phosphate {11XXX} with erythrose-4-phosphate {0000}. Finally, the isotopologue ratio {111000} vs. {111111} represents flux partitioning at the branch point between hexose cycling (entry into glycolysis or PPP) and direct incorporation into starch. Plotting the abundances of the isotopologues {000111}, {110000}, and {111111} as functions of the {111000} isotopologue, respectively, revealed linear relationships in each case (Fig. 7). This demonstrates the high stability of flux partitioning between glycolysis and PPP on the one hand and hexose cycling and incorporation into starch on the other hand. The strongest correlation is detected between the isotopologues {111000} and {000111} ($r^2 = 0.990$), while the ratio between the isotopologues {111000} and {111111} is more variable ($r^2 = 0.723$), identifying direct carbon flux into starch as a slightly more flexible part of carbon metabolism.

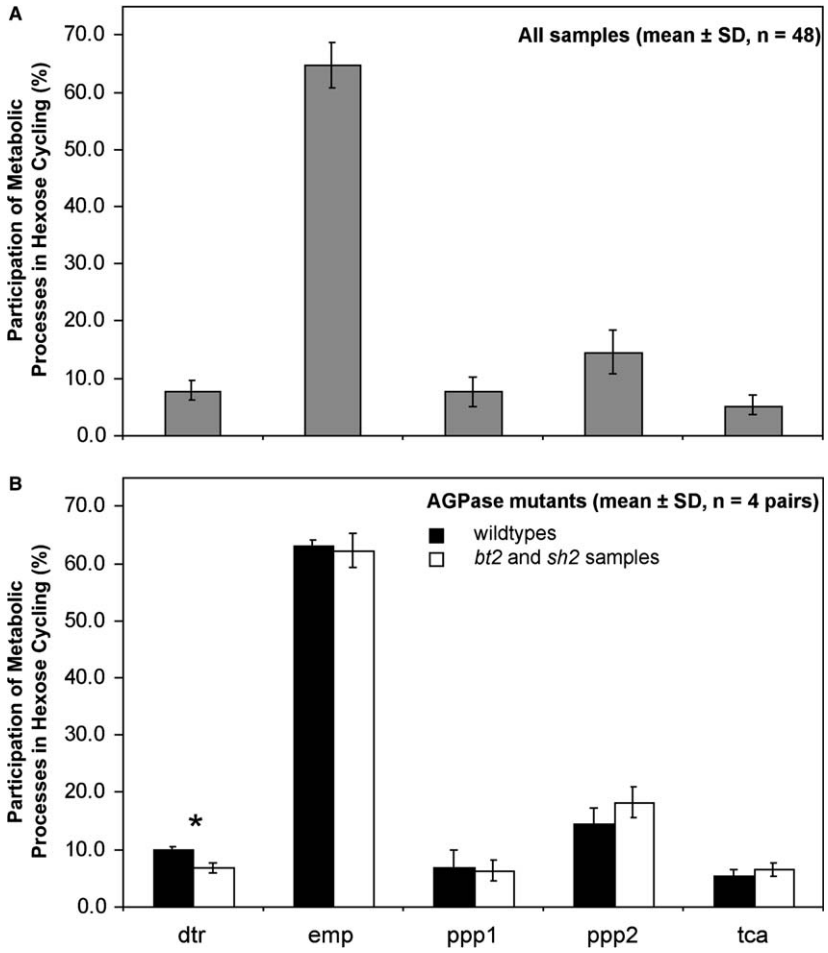

Fig. 6. Quantification of metabolic processes involved in the cycling of hexoses. The fractional participations of five predefined metabolic processes describing the conversion of glucose to glucose were estimated from the excess isotopologue abundances using the 4F software (Ettenhuber et al., 2005). (A) Mean 4F-results of all samples. (B) Mean 4F-results of the AGPase mutants *bt2* and *sh2* in comparison to the mean 4F-results of the corresponding wildtypes. Significantly different means of metabolic processes (p-value < 0.05 in pairwise t-test) are marked with an asterisk. *dtr*, direct transfer of exogenous glucose into starch without prior remodeling; *emp*, reversible conversion of hexose phosphates and triose phosphates via glycolysis/glucogenesis; *ppp1*, full passage through the oxidative and nonoxidative PPP; *ppp2*, reversible exchange flux through the nonoxidative section of the PPP; and *tca*, TCA cycle followed by gluconeogenesis.

2.5. Confirmation of isotopologue patterns by GC-MS

The results reported in this paper are crucially dependent on the accuracy of determining glucose isotopologue concentrations. Therefore, the NMR-derived abundances were independently confirmed for a subset of samples by using GC-MS of Di-*O*-isopropylidene acetate (IPAc) derivatives of glucose (Fig. 8). Mass isotopologue fractions generated by GC-MS or calculated from NMR-derived isotopologue abundances were in good agreement, and the mass isotopologues M+1, M+2, M+3, and M+6 differ on average by 5%, 13%, 7%, and 8%, respectively. M+5 mass isotopologues were constrained to zero level in the analysis of the NMR-data. This is based on the assumption that, due to high isotopic dilution of the ^{13}C-label in our experimental setup, ^{13}C-labeled carbohydrates react only with unlabeled species (see above). Under this condition, glucose isotopologues carrying ^{13}C-atoms on five positions cannot be formed by known reactions of the primary carbohydrate metabolism. In agreement with the above assumption, very low absolute abundances of M+5 mass isotopologues (0.01–0.03 mol%) were observed by GC-MS. Furthermore, between 35% and 100% of this level can be explained by isotopic impurities of the [U-$^{13}C_6$]glucose used here (99 atom% ^{13}C). GC-MS measurements of [U-$^{13}C_6$]glucose revealed that 6.14% of these tracer molecules carry ^{13}C-label at only five positions. Among the glucose molecules that are directly incorporated into starch, this proportion appears as M+5 mass isotopologues. Thus, only very small amounts of M+5 mass isotopologues were generated by synthesis of glucose from two labeled species, and reactions between labeled fragments were negligible. GC-MS analysis also confirmed that *bt2* and *sh2* kernels accumulated lower than wildtype amounts of the {111111} isotopologue, while this level was unchanged in *bt1* and *sh1* kernels (Fig. 8F).

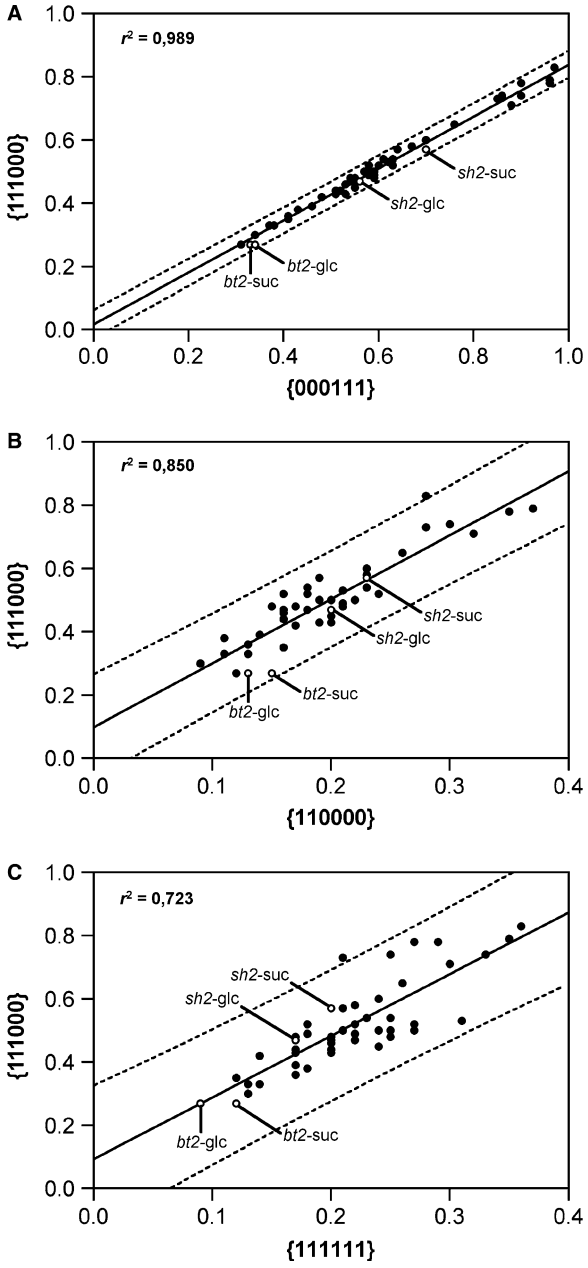

Fig. 7. Correlation between selected isotopologue pairs. The absolute (raw) abundances of the isotopologues {111000} vs. {000111} (A), {111000} vs. {110000} (B), and {111000} vs. {111111} (C) were plotted against each other. The linear regression of the distribution and the 99% prediction band are indicated by solid and dashed lines, respectively.

3. Discussion

The use of stable-isotope labeling under steady state conditions is an emerging method for metabolic flux analysis in plants (Schwender et al., 2004). We used proton-decoupled ^{13}C-NMR spectroscopy to determine the full isotopologue distribution of glucose which was derived from starch. This provided the basis for the analysis of hexose cycling in a heterogenous sample of maize lines including starch-deficient mutants, inbred lines, and crosses which are known to exhibit hybrid vigor. The carbohydrate metabolism involved in hexose cycling was described by assigning specific isotopologues to individual pathways and by applying the 4F software (Ettenhuber et al., 2005). In general, metabolic flux analysis is time-consuming and labour-intensive. Recently, high-throughput methods for flux analysis in microorganisms were developed (Fischer and Sauer, 2003; Wittmann and Heinzle, 2001), and systematic large-scale analyses of metabolic networks are becoming available, e.g. in *Bacillus subtilis* (Fischer and Sauer, 2005) and *S. cerevisiae* (Blank et al., 2005). However, metabolic flux studies in plants are faced with additional difficulties and there are no comparative studies on the effects of different genotypes in plants so far.

For most genotypes, two separate labeling experiments were carried out using [U-$^{13}C_6$]glucose or [U-$^{13}C_{12}$]sucrose, respectively. The natural precursor of starch in maize kernels is photo-assimilated sucrose, which is transported through the phloem and is unloaded into the developing maize endosperm. Gengenbach (1977) first described the method of *in vitro* culture of developing maize kernels using sucrose as a carbon source, but the *in vitro* culture medium also supports the growth on glucose or fructose (Cobb and Hannah, 1986; Cheng and Chourey, 1999; Glawischnig et al., 2002). Both wildtype and mutant maize kernels developed similarly on either carbon source. On sucrose, kernels grew slightly faster than on glucose resulting in a 5–10% increased kernel fresh weight at the end of the labeling period. The *in vitro* culture system supported normal development of the *sh1*, *sh1 sus1*, and *mn1* mutant kernels on medium supplied with either sucrose or glucose. Glucose in the culture medium could not restore wildtype seed phenotype in these mutants, which is in agreement with an earlier report on *mn1* kernels (Cheng and Chourey, 1999). Despite the known regulatory effects of sugars (Koch, 1996), the carbon source in the culture medium had only a minor influence on the isotopologue profile. Even *sh1*, *mn1*, and *sh1 sus1* mutant kernels, in which the interconversion of sucrose and hexoses is affected, had similar glucose isotopologue patterns with glucose or sucrose as carbon sources, respectively (Fig. 2A and C).

3.1. Carbohydrate fluxes and sink strength

Labeling experiments on starch-deficient mutants and hybrid crosses enabled us to investigate the influence of sink strength on relative fluxes through carbohydrate metabolism. Initially, we expected that slowed starch synthesis would lead to increased exposition of hexoses to the reactions of the carbohydrate metabolism and, in turn, to altered glucose labeling patterns. The mutant kernels used in this study show lower starch contents or reduced seed weights, while sink strength in heterotic crosses and in *Sh2-Rev6* kernels is increased. The conserved overall distribution of glucose isotopologues in all genotypes tested here shows that there is no simple correlation between relative fluxes through glycolysis, PPP, or TCA cycle and the

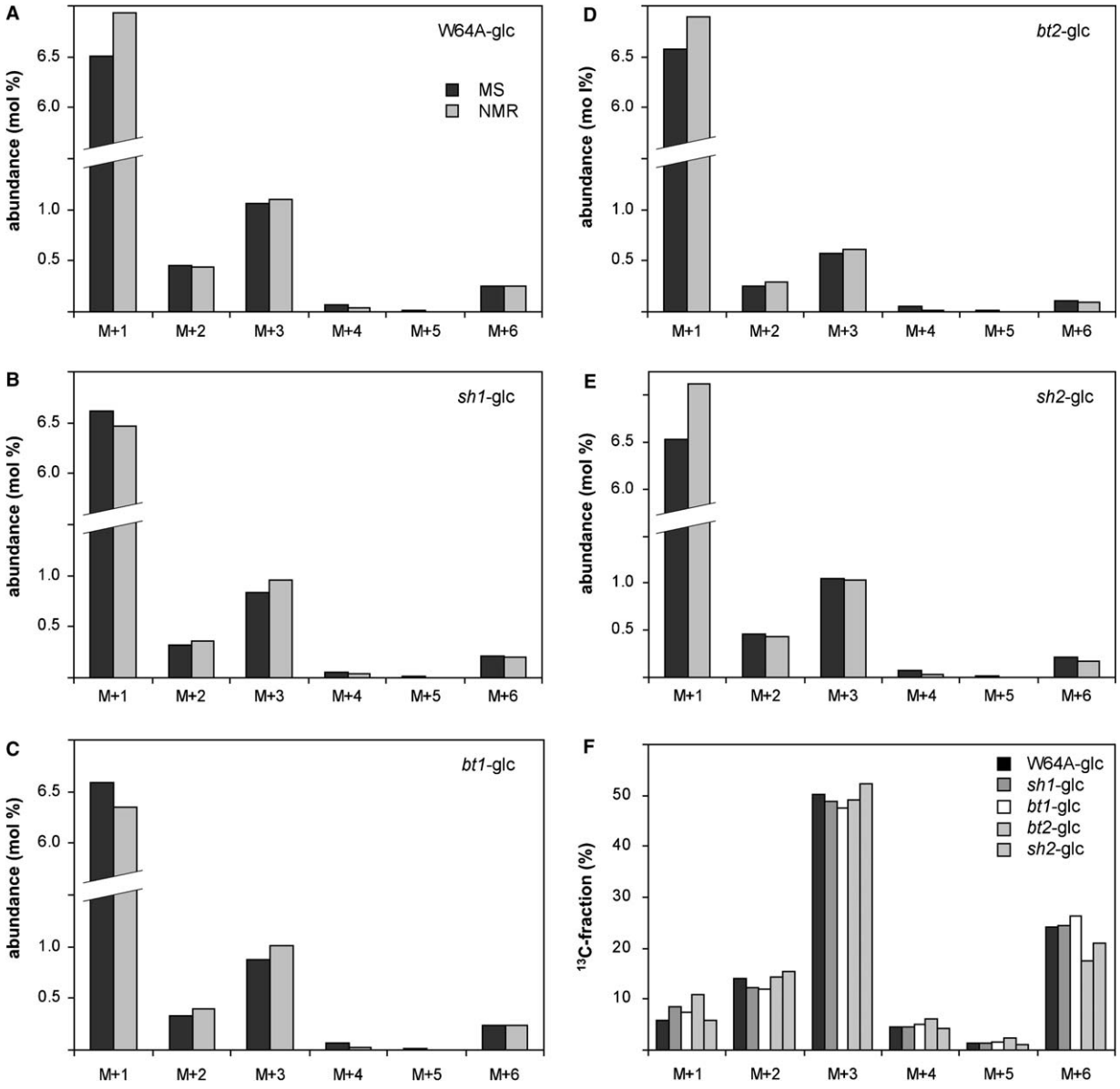

Fig. 8. Comparison of NMR- and MS-derived mass isotopologue abundances. Mass isotopologue abundances of starch-derived glucose from the samples (A) W64A-glc, (B) *sh1*-glc, (C) *bt1*-glc, (D) *bt2*-glc, and (E) *sh2*-glc were determined from GC-MS spectra of IPAc derivatives (black bars) and calculated from glucose isotopologue abundances determined by NMR (grey bars). ^{13}C-fractions of the samples in panels A–E were calculated in order to allow direct comparison of the mass isotopologue data generated by GC-MS (F).

rate of biomass formation or sink strength in maize kernels. A block of AGPase activity (*bt2* or *sh2*) caused an increase in hexose cycling, while a block of ADP-glucose transporter activity (*bt1*) did not. This is surprising given the highly related phenotypes of *bt1*, *bt2*, and *sh2* and the fact that the BT1 transporter acts immediately downstream of AGPase (Fig. 1). One possible explanation is that these mutants have alternative routes for the synthesis of residual starch that involve cytosolic AGPase in *bt1* and plastidial AGPase in *bt2* or *sh2*. This view is supported by experiments on isolated plastids from *bt2* mutant kernels, in which the cytosolic isoform of AGPase is specifically eliminated and ADP-glucose synthesis is accomplished by plastidic AGPase (Denyer et al., 1996). Interestingly, the *bt2* and *sh2* genes were previously found to be involved in the control of kernel composition traits by candidate gene association (Wilson et al., 2004). Our results demonstrate that flux analysis can reveal metabolic phenotypes that could not be predicted based on steady-state levels of metabolites, proteins, or transcripts. This highlights the importance of metabolic fluxes in attempts to integrate 'omics' data and gain a systems-level understanding of plant metabolism.

3.2. Metabolic robustness

Metabolic stability in plants was previously reported for tomato suspension cells at three different culture stages

(Rontein et al., 2002). In agreement with the results of this study, tomato cells showed stable flux ratios at key branch points while fluxes in anabolic pathways, such as polymer synthesis, were low and variable. A speculative explanation for this phenomenon was based on core carbohydrate fluxes that are much faster compared with downstream anabolic pathways. Thus, relative fluxes within the metabolic hub are not affected by varying rates of end-product accumulation.

The glucose isotopologue patterns from ^{13}C-labeled maize kernels indicated high stability of the central carbohydrate metabolism in maize kernels, regardless of carbon source, developmental stage, or sink strength. Specifically, the flux partitioning between glycolysis and PPP was stable and independent of the rate and yield of starch synthesis. These results are consistent with the situation in *B. subtilis*, which showed rigid relative fluxes in mutants of downstream biosynthetic reactions, while lesions within the central carbohydrate metabolism caused significant flux redistributions (Fischer and Sauer, 2005). It should be noted that none of the reactions responsible for scrambling of glucose label are directly affected in the starch-deficient mutants included in this study. By analogy to *B. subtilis*, mutations directly affecting glycolysis or the PPP can be expected to cause flux rerouting in maize kernels. However, there is much greater genetic redundancy in plants compared with microbes. For example, the *Arabidopsis* genome contains multiple copies of genes encoding PPP enzymes (Kruger and van Schaewen, 2003). Due to the additional complexity in plants, a complete block in a given step of the central carbohydrate metabolism may require the inactivation of multiple genes, and the flux-phenotypes of single mutants may be subtle.

In the *Arabidopsis* genome, the largest functional category consists of genes that are implicated in cellular metabolism (The *Arabidopsis* Genome Initiative, 2000). Many of these genes are unique to plants. This highlights the critical importance of metabolism for plants, and in this context the metabolism of sugars is central. It is therefore perhaps of particular interest that we find constant core metabolic fluxes in an organism that is subject to extremes and which, at a cellular level, is remarkably dynamic and plastic. Robustness of living systems was defined as 'the ability to maintain performance in the face of perturbations and uncertainty' (Stelling et al., 2004). The stability of central carbohydrate metabolism may well contribute to the functional robustness of the plant cell.

4. Experimental

4.1. Plant material, kernel culture, and ^{13}C-labeling

Maize plants of the lines W64A, WA64A-*su1-Ref*, W64A-*sh1*, W64A-*bt1*, W64A-*bt2*, W64A-*ae*, W64A-*wx*, Fa56, and Fa56-*Sh2-Rev6* were grown in the field in Gainesville, Florida, in spring 2003. Maize plants of the lines W22, W22-*mn1*, W22-*sh1 sus1*, Fa56, Fa56-*sh2*, Mo17, B73, Mo17 × B73, and B73 × Mo17 were grown in the greenhouse in Freising, Germany, in summer 2003. Ears were harvested 8–10 DPP and kernels were cultured as previously described (Ettenhuber et al., 2005) except that 2,4-dichlorophenoxyacetic acid (2,4-D) was omitted from all media. For labeling, kernel blocks were transferred onto fresh culture media containing 77.4 g/l glucose and 2.6 g/l [U-$^{13}C_6$]glucose or 77.4 g/l sucrose and 2.6 g/l [U-$^{13}C_{12}$]sucrose, respectively. [U-$^{13}C_6$]glucose (99% ^{13}C) and [U-$^{13}C_{12}$]sucrose (99% ^{13}C) were purchased from Isotec, Miamisburg, Florida. Kernels were harvested after 7 days, frozen in liquid nitrogen and stored at −70 °C. For each maize line, kernels from 3 to 5 different plants were labeled and pooled for analysis.

4.2. Isolation of glucose for NMR analysis

Kernels were dried in a lyophilizer for 5 days. Pericarp and embryo were removed by dissection and the endosperm tissue was ground in a mortar with a pestle. Starch was isolated, hydrolyzed by amyloglucosidase to glucose, and glucose was isolated by affinity chromatography as previously described (Ettenhuber et al., 2005). Glucose was further purified by HPLC using a Luna 5 μ NH_2 100 Å column (250 × 21.2 mm, Phenomenex; 40 ml/min, 40 °C), and refractrometric monitoring. Glucose eluted at 8 min in acetonitrile/water 80/20 [v/v]. The solution was evaporated to dryness under reduced pressure and glucose was dissolved in 0.5 ml D_2O for NMR analysis.

Phytoglycogen was extracted with water from 500 mg-aliquots of *su1* endosperm tissue as described by Inouchi et al. (1983). Starch was isolated from the residue after phytoglycogen extraction. The complete degradation of starch or phytoglycogen to glucose by amyloglucosidase, and the subsequent purification of glucose were carried out as described above.

Partial amylolytic hydrolysis of starch granules from [U-$^{13}C_6$]glucose-labeled *su1*-kernels was done as described by Keeling et al. (1988). In this case, starch granules were treated with amyloglucosidase for 60 min without prior gelatinization.

4.3. Measurement of glucose isotopologue abundances by NMR Spectroscopy

^{1}H and ^{13}C NMR spectra were recorded at 500.13 MHz and 125.76 MHz, respectively, using a Bruker DRX500 spectrometer, at 27 °C. The experimental setup, signal assignments, coupling constants and isotope shifts of α- and β-glucose have been reported earlier (Eisenreich et al., 2004). The analysis of ^{13}C abundance and isotopologue composition was performed as described (Eisenreich et al., 2004). Briefly, in the ^{1}H-decoupled ^{13}C NMR spectrum, each line was integrated separately. The relative fractions of each respective satellite pair (corresponding to the relative abundance of certain X groups) in the total signal

integral of a given carbon atom were calculated. These values were then referenced to the global ^{13}C abundance of glucose obtained from isotope ratio mass spectrometry. The ^{13}C abundances of the individual glucose isotopologues were obtained by solving the over-determined linear equation system $\mathbf{D} \cdot i = x$; where i is the vector of isotopologue concentrations, x is the vector of X-group abundances, and $\mathbf{D}$ is the X-group definition matrix. Linear optimization algorithm implemented in Excel Solver was used to get an optimized set of isotopologue concentrations with minimal deviation between experimental and simulated X-group abundances, respectively. Multiple labeled isotopologues which can not be explained by known metabolic pathways were constrained as illegal.

Isotopologues were noted as described (Eisenreich et al., 2004). The carbon skeleton of a metabolite with n carbons is represented by a n-digit binary number where the first digit represents C-1, the second digit represents C-2, etc.; 1 signifies ^{13}C, 0 signifies ^{12}C, and X signifies either ^{12}C or ^{13}C.

Percentage ^{13}C-fractions (f_i) were calculated from the excess enrichment e_i of each isotopologue, the total excess amount t of ^{13}C incorporated into starch during the labeling period, and the number n of ^{13}C atoms of a certain isotopologue by applying $f_i = (n \cdot e_i)/(t \cdot 6)$. For single labeled isotopologues, the excess enrichments e_i were obtained from the molar abundances by subtracting the natural abundance contributions (1.03 mol%). The natural abundances of the multiple labeled isotopologues are in the range between 8.7×10^{-4} and 1.7×10^{-12} mol% and were therefore neglected.

4.4. Isotope ratio mass spectrometry (IRMS)

After NMR analysis, the glucose samples were lyophilized, and global ^{13}C enrichments were determined by isotope ratio mass spectrometry (Isolab GmbH, Germany; Pillonel et al., 2004).

4.5. Measurement of mass isotopologues by GC-MS

1,2:5,6-Di-*O*-isopropylidene-3-acetyl-α-D-glucofuranose (IPAc glucose) was prepared according to Hachey et al. (1999). GC-MS analyses were performed on a GC-17A Gas Chromatograph (Shimadzu, Duisburg, Germany) equipped with a fused silica capillary column (Equity TM-5; 30 m × 0.25 mm × 0.25 μm film thickness; SUPELCO, Bellafonte, PA) coupled to a QP-5000 mass selective detector (Shimadzu, Duisburg, Germany) working in the electron impact (EI) mode at 70 eV. One microliter of a solution containing IPAc glucose was injected in 1:45 split mode at the interface temperature of 260 °C and a helium inlet pressure of 70 kPa. The column was eluted at 150 °C for 3 min and then with a temperature gradient of 10 °C/min to a final temperature of 260 °C that was hold for 3 min. The retention time of IPAc glucose was 8.5 min. Data were collected using the Class 5000 software (Shimadzu, Duisburg, Germany). Selected ion monitoring experiments were carried out on the fragment m/z 287 from the m/z 286 to 295. Selected ion monitoring data were acquired using a 0.3 s sampling rate. Samples were analyzed at least five times. Data evaluation was performed using Microsoft Excel Software. Statistical analysis of the tracer data was done to determine mean, standard deviation and inter sample variance. The ^{13}C enrichment was calculated according to Blom (1988). Theoretical isotope ratio and numerical deconvolution of the data were computed according to Lee et al. (1991) in three steps: determination of the 'IPAc-derivative' spectrum of IPAc glucose, determination of mass isotopomer distribution of the labeled glucose and correction for incorporation of ^{13}C from natural abundance in glucose.

4.6. Statistical analysis of labeling data

Principal component analysis of normalized isotopologue abundances was carried out using XLSTAT software. Paired t-tests, repeated-measures analysis of variance (ANOVA), correlation analysis, and linear regression were performed with Prism4 software (GraphPad).

Acknowledgements

This work was funded by Grants from the Deutsche Forschungsgemeinschaft and the Fonds der Chemischen Industrie. We thank Heidi Miller-Mommerskamp and Claudia Huber for technical support and Fritz Wendling for help with the preparation of the manuscript. We thank Farhah Assaad for helpful discussions and critically reading this manuscript.

Appendix A. Supplementary data

Supplementary data associated with this article can be found, in the online version, at doi:10.1016/j.phytochem.2006.05.035.

References

Bae, J.M., Giroux, M., Hannah, L.C., 1990. Cloning and characterization of the *brittle-2* gene of maize. Maydica 35, 317–322.

Bhave, M.R., Lawrence, S., Barton, C., Hannah, L.C., 1990. Identification and molecular characterization of *shrunken-2* cDNA clones of maize. Plant Cell 2, 581–588.

Birchler, J.A., Auger, D.L., Riddle, N.C., 2003. In search of the molecular basis of heterosis. Plant Cell 15, 2236–2239.

Blank, L.M., Kupfer, L., Sauer, U., 2005. Large-scale ^{13}C-flux analysis reveals mechanistic principles of metabolic network robustness to null mutations in yeast. Genome Biol. 6, R49.

Blom, K.F., 1988. Average mass approach to the isotopic analyses of compounds exhibiting significant interfering ions. Anal. Chem. 60, 966–971.

Boyer, C.D., Hannah, L.C., 2001. Kernel mutants of corn. In: Hallauer, A.R. (Ed.), Specialty Corns, second ed. CRC Press, Boca Raton, FL, pp. 1–31.

Boyer, C.D., Preiss, J., 1978. Multiple forms of starch branching enzyme of maize: evidence for independent genetic control. Biochem. Biophys. Res. Commun. 80, 169–175.

Buchanan, B.B., Gruissem, W., Jones, R.L., 2000. Biochemistry and Molecular Biology of Plants. American Society of Plant Physiology, Rockville, MD.

Cheng, W.-H., Chourey, P.S., 1999. Genetic evidence that invertase-mediated release of hexoses is critical for appropriate carbon partitioning and normal seed development in maize. Theor. Appl. Genet. 98, 485–495.

Cheng, W.-H., Taliercio, E.T., Chourey, P.S., 1996. The *miniature1* seed locus of maize encodes a cell wall invertase required for normal development of endosperm and maternal cells in the pedicel. Plant Cell 8, 971–983.

Chourey, P.S., 1981. Genetic control of sucrose synthetase in maize endosperm. Mol. Gen. Genet. 184, 372–376.

Chourey, P.S., Taliercio, E.W., Carlson, S.J., Ruan, Y.L., 1998. Genetic evidence that the two isozymes of sucrose synthase present in developing maize endosperm are critical, one for cell wall integrity and the other for starch biosynthesis. Mol. Gen. Genet. 259, 88–96.

Cobb, B.G., Hannah, L.C., 1986. Sugar utilization by developing wild type and *shrunken-2* maize kernels. Plant Physiol. 80, 609–611.

Creech, R.G., 1968. Carbohydrate synthesis in maize. Adv. Agron. 20, 275–321.

Denyer, K., Dunlap, F., Thorbjornsen, T., Keeling, P., Smith, A.M., 1996. The major form of ADP-glucose pyrophosphorylase in maize endosperm is extra-plastidial. Plant Physiol. 112, 779–785.

Dieuaide-Noubhani, M., Raffard, G., Canioni, P., Pradet, A., Raymond, P., 1995. Quantification of compartmented metabolic fluxes in maize root tips using isotope distribution from ^{13}C- or ^{14}C-labeled glucose. J. Biol. Chem. 270, 13147–13159.

Doehlert, D.C., Kuo, T.M., 1990. Sugar metabolism in developing kernels of starch- deficient endosperm mutants of maize. Plant Physiol. 92, 990–994.

Doehlert, D.C., Kuo, T.M., 1994. Gene expression in developing kernels of some endosperm mutants of maize. Plant Cell Physiol. 35, 411–418.

Echt, C.S., Chourey, P.S., 1985. A comparison of two sucrose synthetase isozymes from normal and *shrunken-1* maize. Plant Physiol. 79, 530–536.

Eisenreich, W., Ettenhuber, C., Laupitz, R., Theus, C., Bacher, A., 2004. Isotopolog perturbation techniques for metabolic networks: metabolic recycling of nutritional glucose in *Drosophila melanogaster*. Proc. Natl. Acad. Sci. 101, 6764–6769.

Ettenhuber, C., Spielbauer, G., Margl, L., Hannah, L.C., Gierl, A., Bacher, A., Genschel, U., Eisenreich, W., 2005. Changes in flux pattern of the central carbohydrate metabolism during kernel development in maize. Phytochemistry 66, 2632–2642.

Fernie, A.R., Geigenberger, P., Stitt, M., 2005. Flux an important, but neglected, component of functional genomics. Curr. Opin. Plant Biol. 8, 174–182.

Fischer, E., Sauer, U., 2003. Metabolic flux profiling of *Escherichia coli* mutants in central carbon metabolism using GC-MS. Eur. J. Biochem. 270, 880–891.

Fischer, E., Sauer, U., 2005. Large-scale in vivo flux analysis shows rigidity and suboptimal performance of *Bacillus subtilis* metabolism. Nat. Genet. 37, 636–640.

Gengenbach, B.G., 1977. Development of maize caryopses from in-vitro pollination. Planta 134, 91–93.

Giroux, M.J., Boyer, C., Feix, G., Hannah, L.C., 1994. Coordinated transcriptional regulation of storage product genes in the maize endosperm. Plant Physiol. 106, 713–722.

Giroux, M.J., Shaw, J., Barry, G., Cobb, B.G., Greene, T., Okita, T., Hannah, L.C., 1996. A single mutation that increases maize seed weight. Proc. Natl. Acad. Sci. USA 93, 5824–5829.

Glawischnig, E., Gierl, A., Tomas, A., Bacher, A., Eisenreich, W., 2001. Retrobiosynthetic nuclear magnetic resonance analysis of amino acid biosynthesis and intermediary metabolism. Metabolic flux in developing maize kernels. Plant Physiol. 125, 1178–1186.

Glawischnig, E., Gierl, A., Tomas, A., Bacher, A., Eisenreich, W., 2002. Starch biosynthesis and intermediary metabolism in maize kernels. Quantitative analysis of metabolite flux by nuclear magnetic resonance. Plant Physiol. 130, 1717–1727.

Hachey, D.L., Parsons, W.R., McKay, S., Haymond, M.W., 1999. Quantitation of monosaccharide isotopic enrichment in physiologic fluids by electron ionization or negative chemical ionization GC/MS using di-*O*-isopropylidene derivatives. Anal. Chem. 71, 4734–4739.

Hannah, L.C., Giroux, M., Boyer, C., 1993. Biotechnological modification of carbohydrates for sweet corn and maize improvement. Sci. Hortic. 55, 177–197.

Inouchi, N., Glover, D.V., Takaya, T., Fuwa, H., 1983. Development changes in fine structure of starches of several endosperm mutants of maize. Starch 11, 371–376.

James, M.G., Robertson, D.S., Myers, A.M., 1995. Characterization of the maize gene *sugary1*, a determinant of starch composition in kernels. Plant Cell 7, 417–429.

Kanehisa, M., Goto, S., Hattori, M., Aoki-Kinoshita, K.F., Itoh, M., Kawashima, S., Katayama, T., Araki, M., Hirakawa, M., 2006. From genomics to chemical genomics: new developments in KEGG. Nucl. Acid Res. 34, D354–D357.

Katz, J., Rognstad, R., 1967. The labeling of pentose phosphate from glucose-^{14}C and estimation of the rates of transaldolase, transketolase, the contribution of the pentose cycle, and ribose phosphate synthesis. Biochemistry 6, 2227–2247.

Keeling, P.L., Wood, J.R., Tyson, R.H., Bridges, I., 1988. Starch biosynthesis in developing wheat grain. Plant Physiol. 87, 311–319.

Koch, K.E., 1996. Carbohydrate modulated gene expression in plants. Annu. Rev. Plant Physiol. Plant Mol. Biol. 47, 509–540.

Kossmann, J., Lloyd, J., 2000. Understanding and influencing starch biochemistry. Crit. Rev. Plant Sci. 19, 171–226.

Kruger, N.J., Ratcliffe, R.G., Roscher, A., 2003. Quantitative approaches for analysing fluxes through plant metabolic networks using NMR and stable isotope labeling. Phytochem. Rev. 2, 17–30.

Kruger, N.J., van Schaewen, A., 2003. The oxidative pentose phosphate pathway: structure and organisation. Curr. Opin. Plant Biol. 6, 236–246.

Lea, P.J., Chen, Z.H., Leegood, R.C., Walker, R.P., 2001. Does phosphoenolpyruvate carboxykinase have a role in both amino acid and carbohydrate metabolism? Amino Acids 20, 225–241.

Lee, L., Tsai, C.Y., 1985. Effect of sucrose accumulation on zein synthesis in maize starch-deficient mutants. Phytochemistry 24, 225–229.

Lee, W.-N.P., Byerley, L.O., Bergner, E.A., Edmond, J., 1991. Mass isotopomer analysis: theoretical and practical considerations. Biol. Mass Spectrom. 20, 451–458.

Moreno-Gonzales, J., Dudley, J.W., 1981. Epistasis in related and unrelated maize hybrids determined by three methods. Crop Sci. 21, 644–651.

Nelson, O.E., Pan, D., 1995. Starch synthesis in maize endosperms. Annu. Rev. Plant Mol. Biol. 46, 475–496.

Nelson, O.E., Rines, H.W., 1962. The enzymatic deficiency in the *waxy* mutant of maize. Biochem. Biophys. Res. Commun. 131, 297–300.

Pillonel, L., Bütikofer, U., Rossmann, A., Tabacchi, R., Bosset, J.O., 2004. Analytical methods for the detection of adulteration and mislabelling of Raclette Suisse® and Fontina PDO cheese. Mitt. Lebensm. Hyg. 95, 489–502.

Plaxton, W.C., 1996. The organization and regulation of plant glycolysis. Annu. Rev. Plant Mol. Biol. 47, 185–214.

Portais, J.C., Delort, A.M., 2002. Carbohydrate cycling in micro-organisms: what can (13)C-NMR tell us? FEMS Microbiol. Rev. 26, 375–402.

Ratcliffe, R.G., Shachar-Hill, Y., 2001. Probing plant metabolism with NMR. Annu. Rev. Plant Physiol. Plant Mol. Biol. 52, 499–526.

Ratcliffe, R.G., Shachar-Hill, Y., 2006. Measuring multiple fluxes through plant metabolic networks. Plant J. 45, 490–511.

Rontein, D., Dieuaide-Noubhani, M., Dufourc, E.J., Raymond, P., Rolin, D., 2002. The metabolic architecture of plant cells. Stability of central

metabolism and flexibility of anabolic pathways during the growth cycle of tomato cells. J. Biol. Chem. 277, 43948–43960.

Roscher, A., Kruger, N.J., Ratcliffe, G., 2000. Strategies for metabolic flux analysis in plants using labeling. J. Biotechnol. 77, 81–102.

Schwender, J., Ohlrogge, J.B., Shachar-Hill, Y., 2003. A flux model of glycolysis and the oxidative pentose phosphate pathway in developing *Brassica napus* embryos. J. Biol. Chem. 278, 29442–29453.

Schwender, J., Ohlrogge, J., Shachar-Hill, Y., 2004. Understanding flux in plant metabolic networks. Curr. Opin. Plant Biol. 7, 309–317.

Shannon, J.C., Pien, F.-M., Cao, H., Liu, K.-C., 1998. *Brittle-1*, an adenylate translocator, facilitates transfer of extraplastidial synthesized ADP-glucose into amyloplasts of maize endosperm. Plant Physiol. 117, 1235–1252.

Shannon, J.C., Pien, F.-M., Liu, K.-C., 1996. Nucleotides and nucleotide sugars in developing maize endosperms. Plant Physiol. 110, 835–843.

Singletary, G.W., Banisadr, R., Keeling, P.L., 1997. Influence of gene dosage on carbohydrate synthesis and enzymatic activities in endosperm of starch-deficient mutants of maize. Plant Physiol. 113, 293–304.

Sriram, G., Fulton, D.B., Iyer, V.V., Peterson, J.M., Zhou, R., Westgate, M.E., Spalding, M.H., Shanks, J.V., 2004. Quantification of compartmented metabolic fluxes in developing soybean embryos by employing biosynthetically directed fractional ^{13}C labeling, two-dimensional [^{13}C, ^{1}H] nuclear magnetic resonance, and comprehensive isotopomer balancing. Plant Physiol. 136, 3043–3057.

Stelling, J., Sauer, U., Szallasi, Z., Doyle 3rd., F.J., Doyle, J., 2004. Robustness of cellular functions. Cell 118, 675–685.

Sullivan, T.D., Kaneko, Y., 1995. The maize *brittle 1* gene encodes amyloplast membrane polypeptides. Planta 196, 477–484.

Szyperski, T., 1995. Biosynthetically directed fractional ^{13}C-labeling of proteinogenic amino acids. An efficient analytical tool to investigate intermediary metabolism. Eur. J. Biochem. 232, 433–448.

Tetlow, I.J., Morell, M.K., Emes, M.J., 2004. Recent developments in understanding the regulation of starch metabolism in higher plants. J. Exp. Bot. 55, 2131–2145.

The *Arabidopsis* Genome Initiative, 2000. Analysis of the genome sequence of the flowering plant *Arabidopsis thaliana*. Nature 408, 796–813.

Tobias, R.B., Boyer, C.D., Shannon, J.C., 1992. Alterations in carbohydrate intermediates in the endosperm of starch-deficient maize (*Zea mays* L.) genotypes. Plant Physiol. 99, 146–152.

van Winden, W., Verheijen, P., Heijnen, S., 2001. Possible pitfalls of flux calculations based on (13)C-labeling. Metab. Eng. 3, 151–162.

Wang, Y.-J., White, P., Pollack, L., Jane, J.-L., 1993. Characterization of starch structures of 17 maize endosperm mutant genotypes with Oh43 inbred line background. Cereal Chem. 70, 171–179.

Wilson, L.M., Whitt, S.R., Ibanez, A.M., Rocheford, T.R., Goodman, M.M., Buckler IV, E.S., 2004. Dissection of maize kernel composition and starch production by candidate gene association. Plant Cell 16, 2719–2733.

Winter, H., Huber, S.C., 2000. Regulation of sucrose metabolism in higher plants: localization and regulation of activity of key enzymes. Crit. Rev. Plant Sci. 19, 31–67.

Wittmann, C., Heinzle, E., 2001. Application of MALDI-TOF MS to lysine-producing *Corynebacterium glutamicum*: a novel approach for metabolic flux analysis. Eur. J. Biochem. 268, 2441–2455.

Wolf, D.P., Hallauer, A.R., 1997. Triple testcross analysis to detect epistasis in maize. Crop Sci. 37, 763–770.